Complementary SRR-Based Reflector to Enhance Microstrip Antenna Performance

Mustafa H. B. Ucar

Information Systems Engineering Department
Kocaeli University, Umuttepe Campus, 41001 Kocaeli, Turkey
mhbucar@kocaeli.edu.tr

Abstract — In this paper, complementary split ring resonator (SRR) based reflector to enhance the printed slot dipole (PSD) antenna performance is introduced. The numerically calculated return-loss, directivity and radiation pattern results of the PSD antenna, with (w/) and without (w/o) CSRR element etched on reflector plane are presented and investigated. Numerical analysis and modelling of the proposed design are carried out using CST Microwave Studio simulator based on the finite integration technique. According to the simulation results, with the inclusion of the CSRR-based reflector into the PSD antenna, the directivity is increased by values changes from 0.6 dB to 4.25 dB through the operation band, while an improvement in bandwidth (~2.1%) is seen. It is also shown that this improvement in antenna performance is due to the ε-negative (ENG) behavior of CSRR structures. Prototype of the proposed antenna is fabricated using Arlon DiClad 880 substrate with electrical permittivity of ε_r= 2.2. A quite good agreement between simulation and measurement is obtained. In this study, it is shown that the radiation performance of the antenna can be increased easily by using the CSRR element as a reflector in the antenna structure with a new enhancement approach. Also, the proposed antenna with a compact size of $0.27\lambda \times 0.41\lambda$ is appropriate for operating in IEEE 802.11b/g/n/ax (2.4 GHz) WLAN applications.

Index Terms — Complementary split ring resonator, microstrip antennas, reflector, split ring resonator.

I. INTRODUCTION

Microstrip antennas are widely preferred due to their low-profile, lightweight and easy fabrication, in many applications. On the other hand, it is also well known that, conventional microstrip antennas are featured with their disadvantages such as narrow bandwidth, lover gain and lower power-handling capability [1, 2]. In this context, a series of studies involving changes in either the antenna element or the ground plane or the feed structure to increase the antenna radiation performance are included in the literature [3–19]. Many enhancement techniques such as including parasitic elements [3–5], modifying antenna [6–7], using metasurfaces [8–12], superstrates [13–15] and utilizing band gap [16, 17] or defected ground structures [18, 19] are also reported in these studies. However, many of these techniques increase the complexity and also the size of the antenna, which makes physical realization difficult. In this context, metamaterials has played an important role in reducing the complexity caused by the addition of extra structures, as well as improving the performance of antenna. As is known to all, SRR structures were originally introduced as metamaterial structures showing μ-negative behavior, which have band stop characteristic in a certain frequency band [20]. Moreover according to Babinet's principle, it is also shown that by utilizing a complementary SRR (CSRR), a band-pass performance can be ensured [21, 22]. Recently, SRRs and CSRRs have been used as an antenna radiation element [5−7], artificial substrate [8−10] and also placed on feeding structure [6] or ground plane [10] to enhance antenna performance. In [5] a dual-band loop-loaded printed dipole antenna with a wideband microstrip balun structure is introduced for 3/5.5 GHz WiMAX applications. In that study, triple-band performance is achieved by improving the return loss performance with the inclusion of the parasitic SRR element in to the antenna structure. In another work [6], a multiband monopole antenna based on CSRR was presented, which covers WLAN and WiMAX frequency bands. Also in that study, CSRRs are used side by side as the main radiator of the antenna to keep the antenna size small. By using the filtering characteristics of the penta-ring SRR element multiband antenna performance was also provided [7]. An artificial substrate composed of SRR elements was proposed for a microstrip patch antenna to provide frequency tuning as well as miniaturization [8].

Table 1: Summary of enhancement techniques for printed antennas using SRR/CSRR structures

Ref. No.	Operation	Adjustment				Enhancement		
		On/In	Technique	Element		BW	Directivity	Efficiency
[5]	Multi-band	Antenna	Loading	SRR		✗	✗	✗
[6]	Dual-band	Antenna	Modifying	CSRRs		✗	N/A	N/A
[7]	Multi-band	Antenna	Modifying	SRR		N/A	N/A	N/A
[8]	Single-band	Substrate	Modifying	SRR		✗	✓	✗
[9]	Single-band	Substrate	Loading	3D-SRR		✓	✗	N/A
[10]	Single-band	Feeding	Loading	SRR		✓	N/A	N/A
[11]	Multi-band	Ground	Modifying	CSRR		N/A	N/A	N/A
[12]	Dual-band	Ground	Modifying	CSRR		✗	✗	N/A
This work	Single-band	Reflector	Etching	CSRR		✓	✓	✓

N/A denotes that the related performance evaluation "not available" in that paper.

Metamaterials were also used to design electrically large property (ELP) antennas [9]. With the ELP method relatively high gains can be obtained in the same physical dimensions while increasing the bandwidth by using ENG featured metamaterials. However, the proposed array with ELP is of a complexity that can be difficult during the fabrication. In [10], for better impedance bandwidth and to achieve circular polarization, dual SRR elements are placed on the backside of the slot antenna, i.e. the feed plane. In addition, the CSRR structure is etched into the ground plane of the fractal microstrip antenna to achieve multi-band performance [11]. Furthermore, CSRR structures are also incorporated into the multilayer metasurface (MS) design to realize the dual-band operation [12]. On the other hand, in that study fabrication challenges were encountered due to the lamination of the multiple substrates to each other in the production of the proposed layered MS geometry. A detailed summary of enhancement techniques for printed antennas using SRR/CSRR structures are listed in Table 1. Unlike from previous designs reported in literature [5–12], the printed slot dipole antenna (PSD) introduced in this paper utilizes the complementary SRR element as a reflector to enhance the radiation performance. Compared to the aforementioned studies, here the CSRR structure was used in antenna design by etching on the reflector plane at a certain distance from the antenna, with a simplistic approach in terms of modeling and manufacturing. Also, apart from the previously reported literature [6, 11, 12], the use of the CSRR element in the reflector improves the bandwidth performance while providing a slight increase in the directivity and efficiency of the proposed PSD antenna as depicted in Table 1.

In the paper, CST based simulations [23] including the radiation performances, (such as bandwidth, directivity and efficiency) along with the corresponding return loss measurement of the PSD antenna with (w/) and without (w/o) CSRR element etched on reflector are presented and discussed. According to the simulation

and measurement results, when the CSRR element is etched on the reflector of the PSD antenna, while a relatively improvement in bandwidth (~2.1%) was observed, the directivity was also increased by at least 0.6 dB through the operation band. In addition, a slightly increase in antenna efficiency was also seen.

The outline of the paper is organized as follows. Section 2 describes the printed slot dipole (PSD) antenna design with CSRR-based reflector and the intended use of the CSRR in the reflector. In Section 3, the numerical analysis results of the PSD antenna with CSRR-based reflector design are given and discussed. Also in Section 3, the effects of optimized parameters on the radiation performance, such as the dimensions of the PSD, and CSRR elements and the distance of the reflector to the antenna plane are included. In Section 4, the electrical behavior of the CSRR structure through the operating band is examined and its contribution to the improvement of antenna performance is discussed, and finally, the paper is summarized with concluding remarks in Section 5.

II. ANTENNA DESIGN

The proposed microstrip-line coupled printed slot dipole (PSD) antenna with CSRR-based reflector and its detailed views along with physical parameters are shown in Fig. 1 and Fig. 2 respectively. As can be seen, the design consists of stepped microstrip line-fed slot dipole element and CSRR-based reflector to enhance radiation performance of the PSD antenna. The PSD element and microstrip feed line are etched each side of an Arlon DiClad 880 substrate that cover an area of 34×52 m^2 with dielectric constant of ε_r=2.2 and thickness of t=0.76 mm. The PSD antenna is excited by a stepped microstrip line placed on the other side of the dielectric substrate. The feedline is designed to have two sections with 50Ω $(w_f \times l_f)$ and ~40 Ω $(w_s \times l_s)$ characteristic impedances, so as to ensure a better impedance matching. As shown in Fig. 1, the concentrically placed CSRR elements are etched on metallic reflector and located underneath the

PSD antenna element at a distance of h=11.5 mm. The slits on outer and inner slots of the CSRR are located perpendicular to the PSD element towards the upper and lower edges of the reflector, respectively.
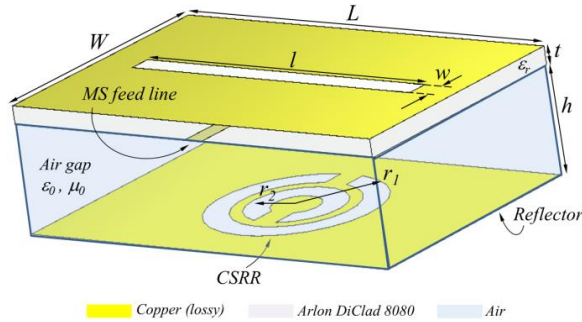

Fig. 1. The proposed MS-line fed PSD antenna with CSRR-based reflector: L=52, W=34, l=40.5, w=3, t=0.76, h=11.5, r_1=10.9, r_2=6.1, all in mm ε_r=2.2.
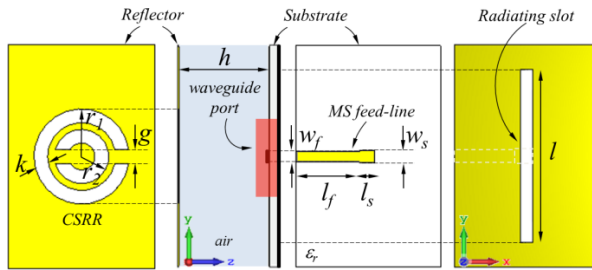

Fig. 2. The detailed views and physical parameters of the proposed PSD antenna with CSRR-based reflector: k=g=3.15, r_1=10.95, r_2=6.1, h=11.5, w_f =2.4, l_f =15, w_s=3, l_s=3.5 all in mm, ε_r=2.2.

The CSRR structure having band-pass filter characteristics over a certain frequency range is a well-known meta-material. Different from the previously reported methods of using SRR/CSRR structures to improve antenna performance in the literature [5−12] in this study, the CSRR is used as a reflector located at a certain distance (h) from the antenna structure to improve the antenna performance in terms of both bandwidth and directivity. Compared to the aforementioned studies, here the CSRR structure was utilized in antenna design by etching on the reflector placed at a certain distance from the antenna, with a simplistic approach in terms of modeling and manufacturing. The interaction of the CSRR structure with the electric field results in occurrence of strong dispersion at the resonance frequency and correspondingly CSRR provides negative dielectric permittivity at the resonance frequency. In this context, to improve the radiation and bandwidth performance of the PSD antenna by creating a new resonance near the resonance frequency of the PSD antenna, firstly the CSRR structure is sized to resonate

around 2.4 GHz. During the design process, while achieving the ultimate CSRR-based reflector backed PSD antenna, the dimensions of the PSD ($w \times l$) and CSRR elements (k, g, r_1, r_2) and the distance of the reflector to the antenna plane (h) were set as critical design parameters and optimized.

III. RESULTS AND DISCUSSION

The simulated return loss performances of the PSD antenna, utilizing reflector with (w/) and without (w/o) CSRR are displayed in Fig. 3. As seen, while the fully metallic reflector (w/o CSRR) backed PSD has a resonance around 2.4 GHz with a bandwidth of 2.5%, the inclusion of the CSRR into reflector leads to a ~2.1% increase in bandwidth around 2.38 GHz without deteriorating the antenna radiation performance as seen in Fig. 4. The simulated radiation patterns of the PSD antenna backed reflector with and without CSRR at 2.4 GHz are depicted in Fig. 4. It shows that the proposed CSRR-based reflector backed PSD design has an omni-directional pattern for H-plane and bi-directional pattern for E-plane. Furthermore, the inclusion of CSRR into the reflector does not have any detrimental effect on the antenna radiation performance.
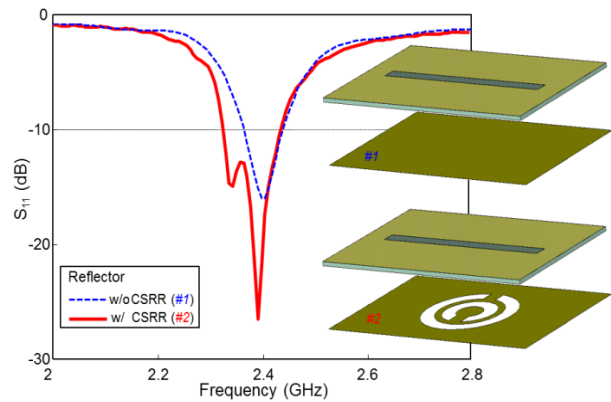

Fig. 3. The simulated return loss performances of the PSD antenna using reflector with (w/) and without (w/o) CSRR.
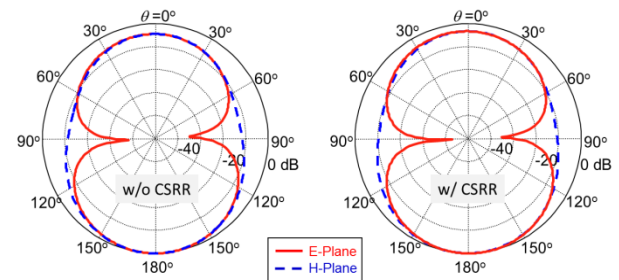

Fig. 4. The normalized radiation patterns of the PSD antenna using reflector with (w/) and without (w/o) CSRR at 2.4 GHz.

In order to validate the simulation results, a prototype of the proposed CSRR-based reflector backed PSD antenna was fabricated on an Arlon DiClad 880 substrate (ε_r= 2.2, h=0.79) according to the optimized design parameters in Fig. 2. A photograph of the fabricated antenna is shown in Fig. 5. The measured and simulated return loss characteristics are presented in Fig. 6. As can be seen in Fig. 6, there is a good agreement between the return loss simulation and measurement results, except for slight differences due to fabrication and material losses. Also measurement reveals that antenna with CSRR etched reflector has impedance bandwidth of 110 MHz (S_{11}<−10 dB) 2.32– 2.43 GHz, and is slightly greater than stand-alone reflector backed one. The designed antenna with a compact size of $0.27\lambda \times 0.41\lambda$ is appropriate for operating in IEEE 802.11b/g/n/ax (2.4 GHz) WLAN applications covering 2.32 GHz – 2.43 GHz frequency band. In addition, radiation pattern measurements were performed in an anechoic chamber using the De0530 model horn antenna (0.5-30 GHz developed by Diamond Engineering) with the measurement setup shown in Fig. 7. A Rohde & Schwarz ZVB 20 VNA as well as low loss coaxial cables were used in these measurements. The measured patterns along with the simulations at the operational frequency of 2.4 GHz are shown in Fig. 8, where a good agreement except tolerable discrepancies is observed. The measured gain of the PSD antenna design in which the CSRR-based reflector is included is 3-5.5 dBi in the relevant band. Also note that the inclusion of the CSRR reflector structure provides at least 1dB increase in gain values compared to the design without the CSRR-based reflector.
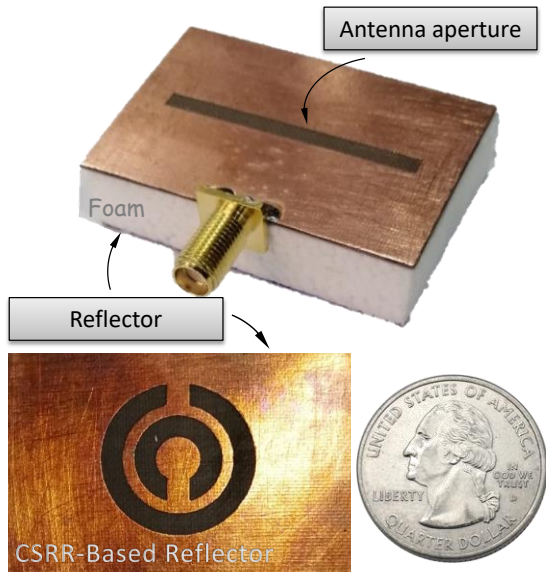

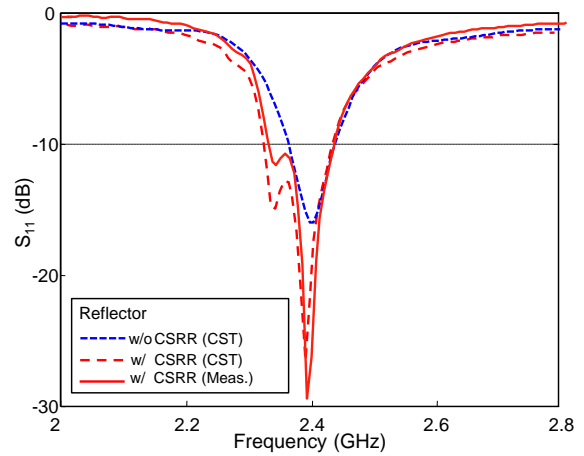Fig. 5. The perspective and back views of the fabricated PSD antenna with CSRR-based reflector.

Fig. 6. The simulated and measured return loss performances of the PSD antenna using reflector with (w/) and without (w/o) CSRR.

Fig. 7. The measurement setup of the proposed PSD antenna with CSRR-based reflector.
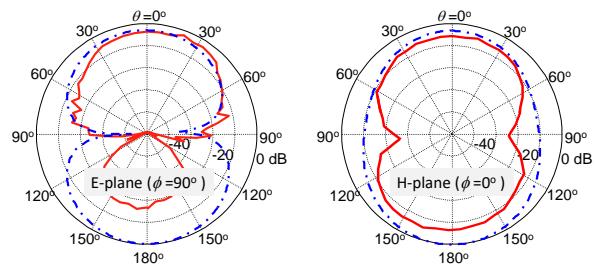

Fig. 8. The measured and simulated radiation patterns of the PSD antenna with CSRR-based reflector at 2.4 GHz.

While etching the CSRR element to the reflector, it was primarily aimed to generate an additional resonance near the operating frequency of the PSD antenna. Thus, these two adjacent bands are joined together by optimizing

the aforementioned critical design parameters and a rather larger bandwidth performance is provided. During the design process, besides the improvement in the bandwidth, some enhancements were also observed in both the directivity and efficiency. To demonstrate the effect of the CSRR based reflector on the antenna directivity, the simulated directivity performance of the PSD antenna utilizing reflector w/ and w/o CSRR through the operation band is depicted in Fig. 9. As can be seen, the inclusion of the CSRR into the reflector results in increases in the directivity which vary from 0.6 dB to 4.5 dB through the operation bands.
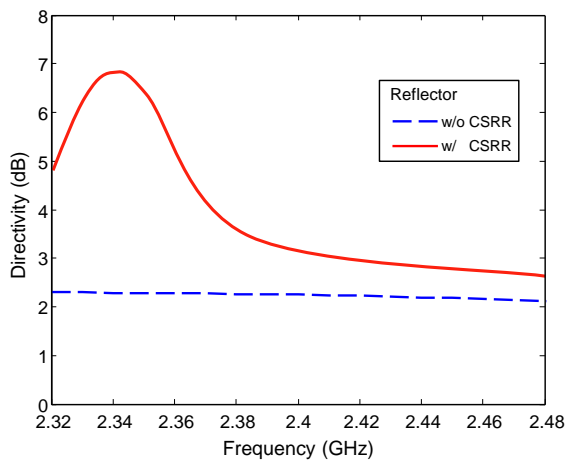

Fig. 9. The simulated directivity performances of the PSD antenna using reflector with (w/) and without (w/o) CSRR through the operation band.
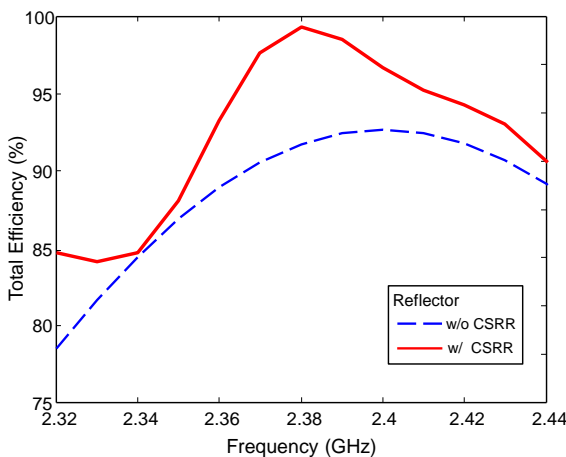

Fig. 10. The calculated total efficiency of the PSD antenna using reflector with (w/) and without (w/o) CSRR through the operation band.

As it is well-known, the total efficiency (e_0) of the antenna is used to account for losses such as reflection (mismatch), conduction and dielectric losses. These losses directly affect the gain of the antenna, thus the radiation performance. In this context to examine the effect of the CSRR on the antenna efficiency performance, the total efficiency of the PSD is calculated and the results are given in Fig. 10. As seen, the inclusion of CSRR in to the reflector causes an increase, especially at the upper frequencies. It is noted that the calculated efficiency of the PSD antenna with CSRR-based reflector through the operation band is at least 83%. The improvements observed in antenna radiation performance with the incorporation of the CSRR element into the reflector are summarized in Table 2.

Table 2: The summary of enhancements in the radiation performances of the PSD antenna with incorporation of the CSRR in to the reflector

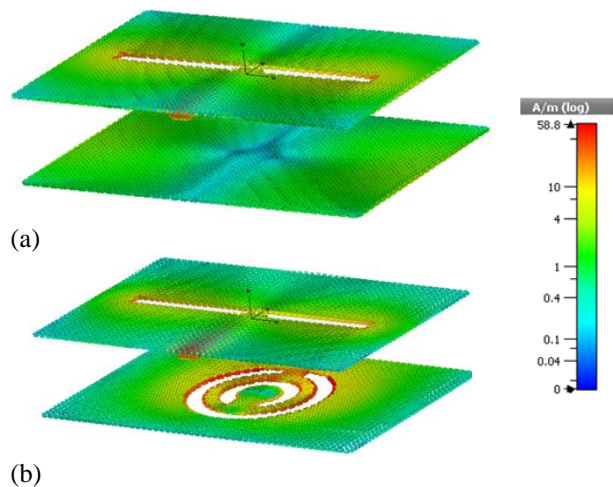|		CSRR		Changes
		w/o	w/	
Performances	**Bandwidth (MHz)**	60 (2.5%)	110 (4.6%)	50 (2.1%) ↑
	Directivity (dB)	2.1~2.3	2.8~6.8	0.6~4.5↑
	Efficiency (%)	78~92	83~98	1~8 ↑

Fig. 11. Surface current distribution of the PSD antenna at 2.38 GHz: (a) stand-alone reflector, and (b) CSRR etched reflector.

The computed surface current distribution of the PSD antenna at the 2.38 GHz is shown in Fig. 11 to endorse the effect of the CSRR-based reflector on the antenna radiation performance. As can be seen, in absence of the CSRR element on the reflector surface (w/o CSRR, i.e., Fig. 11 (a)), the current distribution at 2.38 GHz is mainly concentrated over the PSD element. On the other hand, in presence of the CSRR element

on the reflector surface (w/ CSRR, i.e., Fig. 11 (b)), the distribution at 2.38 GHz is observed predominantly around the PSD as well as the inner and out loops of the CSRR element. Indeed, these results support that the upper and the lower bands of the operation frequency band centered 2.38 GHz occur by means of PSD antenna and CSRR elements, respectively. As a result, by placing the CSRR element on the reflector surface, a secondary resonance is obtained due to the strong resonant behavior of the CSRR structure; thus, the impedance bandwidth is relatively increased (~ 2.1%).

In antenna design section while achieving the ultimate CSRR-based reflector backed PSD antenna design, it was stated that some of the physical dimensions of the proposed antenna are the crucial design parameters that directly affect the antenna radiation performance. For an efficient design process, it is very important and helpful to reveal these important parameters effect, and especially to associate the geometrical parameters with the operation band. Accordingly, in this section, the effects of the aforementioned critical design parameters such as the length of the slot (l), gaps width (g) and outer ring radius (r_1) of the CSRR and the distance of the reflector to the antenna plane (h) on the antenna return loss performance are also examined. It is noted that, during parametric studies, only one parameter was changed at a time, while the others were preserved constant.

As seen Fig. 12 (a), while the slot length directly contributes the occurrence of the resonance frequency around the 2.4 GHz, it also plays an important role in the creating of an additional resonance in vicinity of the first resonance with the CSRR based reflector. Hence, a considerably large bandwidth is provided by specifying the slot length as 40.5 mm with optimized design parameters. Also, the distance of the CSRR based reflector to the antenna plane is set 11.5 mm to ensure better impedance matching and to achieve the desired broadband performance through the operation band as shown in Fig. 12 (b). In addition, a series of parametric studies were also carried out for the two critical design parameters of CSRR geometry that affect the radiation performance, namely the gap width (g) and the outer ring radius (r_1) and presented in Fig. 12 (c) and Fig. 12 (d) respectively. As shown in Fig. 12 (c), when the gap width of the CSRR is increased from 3 mm to 3.9 mm, the lower resonance due to the CSRR element shifts slightly upward. By setting the gap width as 3.15 mm, better impedance matching is achieved and desired relatively wideband performance realized. In Fig. 12 (d), the effect of the CSRR's outer ring radius (r_1) on the simulated S_{11} performance is shown. It is observed that the outer radius of the CSRR is increased from 10.45 mm to 10.95 mm, the lower resonance due to the CSRR element shifts slightly downward.
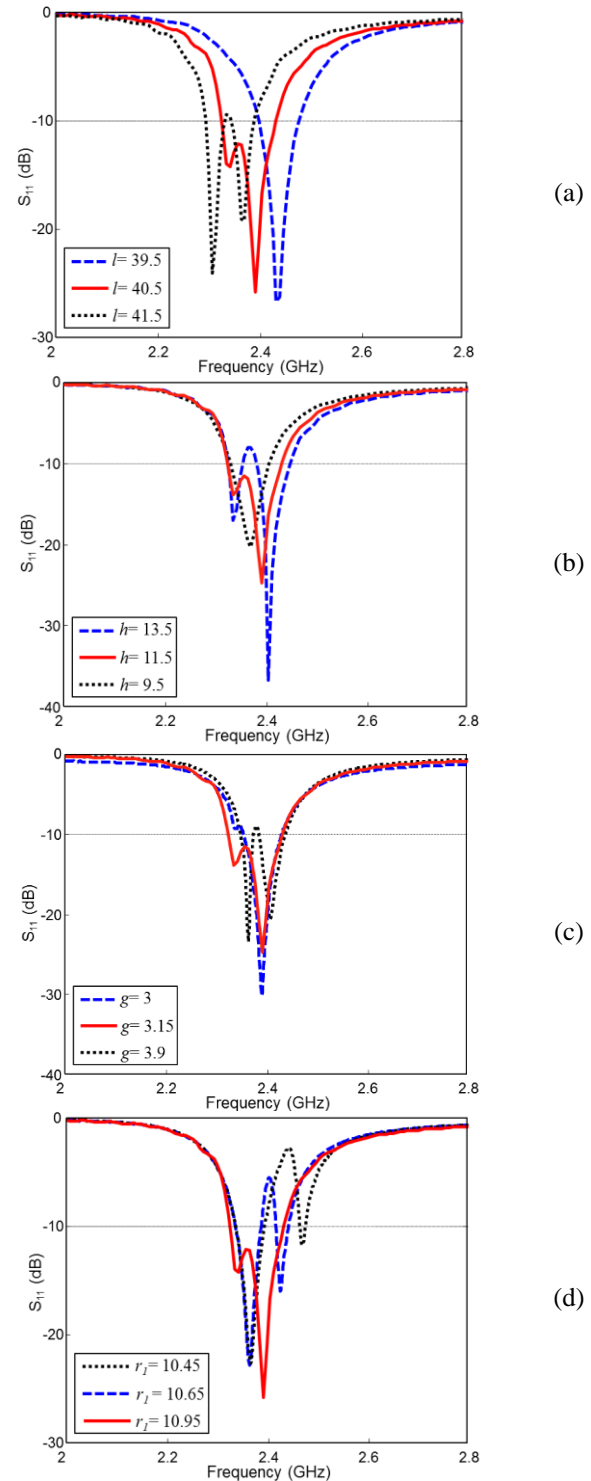

Fig. 12. The effects of critical design parameters on the return loss performance of the proposed CSRR-based reflector backed PSD antenna: (a) slot length; l, (b) distance of the CSRR-based reflector to the antenna plane; h, (c) CSRR's gap width; g, and (d) outer ring radius of the CSRR; r_1, (all in mm).

As a result, according to Fig. 12, it can be stated that while the dipole length mainly controls the fundamental resonance which is centered 2.4 GHz, the CSRR-based reflector plays a key role in occurrence of the additional resonance at the lower frequency. Thus, with the optimization of the relevant physical dimensions, the gap between the lower and upper resonances has been closed and joined to provide a greater bandwidth performance. Also, slot and CSRR dimensions appear to play an important role in improving impedance matching at the operation band for desired rather broadband performance.

IV. ELECTRICAL BEHAVIOUR OF THE CSRR-BASED REFLECTOR

In the previous sections, it is numerically shown that the enhancements in the antenna radiation performances such as bandwidth, directivity and efficiency are mainly due CSRR structure etched on the reflector plane. The interaction of the CSRR structure with the electric field results in occurrence of strong dispersion at the resonance frequency and correspondingly CSRR provides negative dielectric permittivity at the resonance frequency. Actually, those improvements are due to the inherent features of metamaterials, i.e., CSRR structure etched on the reflector plane. To prove that, those improvements in antenna performance is due to the ε-negative (ENG) behavior of the CSRR structures, the scattering parameters (transmission- S_{21} and reflection-S_{11}) of the CSRR element in the respective operation band are first examined. The simulated scattering parameters of the CSRR-based reflector along with the simulated waveguide setup are depicted in Fig. 13. In the S-parameter simulations of the CSRR element, the ports (Port-1 and Port-2) are defined along the z-plane at appropriate distances from the CSRR in the waveguide. The boundaries are also specified for the boundary conditions. The CSRR structure is excited by the plane wave to the Port-1, and the simulated transmission and reflection parameters are extracted from the Port-2. As can be seen from Fig. 13, the CSRR structure exhibits band-pass filter performance around 2.4 GHz Then, using the simulated scattering parameters effective medium parameters (ε_{eff}, μ_{eff}) of the CSRR are also numerically extracted using robust method reported in [24]. According to this method, first the effective refractive index n and impedance Z are obtained through the S parameters calculated from a wave incident normally on CSRR-based reflector. n is defined in terms of transmission (S_{21}) and reflection (S_{11}) parameters as follows:

$$n = \frac{1}{kd}cos^{-1}\left[\frac{1}{2S_{21}}(1 - S_{11}^2 + S_{21}^2)\right], \quad (1)$$

where k and d denote wave number of the incident wave and the thickness of the CSRR-based reflector,

respectively. Also, Z is determined from the scattering parameters as follows:

$$Z = \sqrt{\frac{(1+S_{11})^2 - S_{21}^2}{(1-S_{11})^2 - S_{21}^2}}. \quad (2)$$

Later, the permittivity ε_{eff} and permeability μ_{eff} are calculated using relations:

$$\mu_{eff} = nZ, \qquad \varepsilon_{eff} = n/Z. \quad (3)$$

For metamaterials with resonant characteristics, there is always a frequency region where the branches related with the inverse cosine of equation (1) get too close together and it becomes difficult to get the exact solution. In the study, a more stable and accurate retrieval was achieved with the CST-based result template which utilize the algorithm of the method proposed in [24].
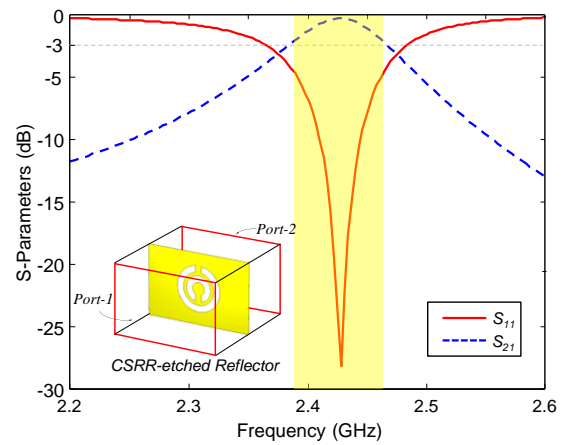

Fig. 13. The simulated scattering parameters of the CSRR-based reflector along with the simulated waveguide setup.
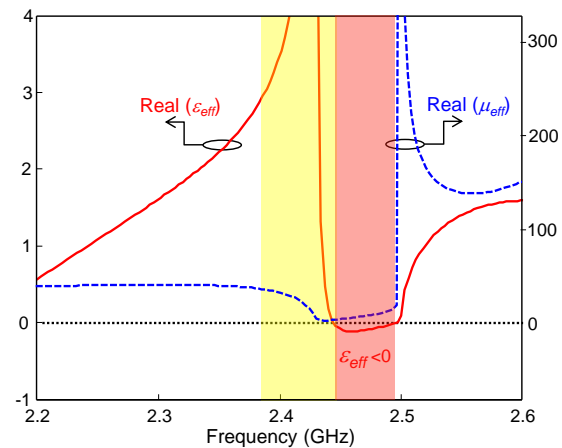

Fig. 14. The extracted material parameters for the CSRR-based reflector considered in Fig. 13.

The extracted material parameters for the CSRR-based reflector using scattering parameters in Fig. 13 are

depicted in Fig. 14. As seen in Fig. 14, while the CSRR exhibits a negative effective permittivity (ENG) above the resonance frequency, the CSRR has a positive effective permittivity below the resonance frequency. These results confirm the effect of the filtering performance of the CSRR-based reflector improving both the bandwidth and directivity of the PSD antenna. Thus, while creating a new resonance with the CSRR based reflector, it can be said that the CSRR structure, with the ε-negative behavior, contributes to the improvement of the antenna performance in terms of the bandwidth, directivity and efficiency.

VI. CONCLUSION

A complementary split ring resonator (CSRR) based reflector to enhance the printed slot dipole (PSD) antenna performance has been presented. In the paper, it is shown that employing the proposed CSRR-based reflector in the geometry of the antenna, the bandwidth and directivity performances of the antenna are enhanced with a simplistic design approach. A prototype of the proposed antenna has been fabricated and a fairly good agreement between simulation and measurement was observed. Measurement reveals that antenna with CSRR etched reflector has impedance bandwidth of 110 MHz ($S_{11}<-10$ dB) 2.32– 2.43 GHz, and is slightly greater than stand-alone reflector backed one. According to the simulation and measurement results, when the CSRR-based reflector was etched on the reflector of the PSD antenna, an improvement in bandwidth (~2.1%) was observed while the directivity and the efficiency were increased by at least 0.6 dB and 1% respectively. In addition, the material properties of the CSRR was extracted and examined. Accordingly, it has been shown that those improvements are due to the metamaterial properties of the CSRR structure, i.e., ε-negative (ENG) feature. It has been also shown with the parametric studies that CSRR dimensions and slot length have critical effects on the achieving greater bandwidth. The proposed antenna with a compact size of $0.27\lambda \times 0.41\lambda$ is appropriate for operating in 2.4 GHz WLAN applications. Besides, this simplistic approach can be easily applied to antenna structures in various wireless communication systems.

ACKNOWLEDGMENT

REFERENCES

[1] R. Garg, P. Bhartia, I. Bahl, and A. Ittipiboon *Microstrip Antenna Design Handbook*, Artech House, Reading, MA, 2001.

[2] G. Kumar and K. P. Ray, *Broadband Microstrip Antenna*, Norwood, MA, 2003.

[3] S. Peddakrishna, T. Khan, and B. K. Kanaujia, "Resonant characteristics of aperture type FSS and its application in directivity improvement of microstrip antenna," *AEU- International Journal of Electronics and Communications*, vol. 79, pp. 199-206, Sept. 2017.

[4] M. H. B. Ucar, A. Sondas, and Y. E. Erdemli, "Dual-band loop-loaded printed dipole antenna with a wideband microstrip balun structure," *Applied Computational Electromagnetics Society (ACES) Journal*, vol. 27, no. 6, pp. 458-465, June 2012.

[5] M. H. B. Ucar and Y. E. Erdemli, "Triple-band microstripline-fed printed wide-slot antenna for WiMAX/WLAN operations," *Applied Computational Electromagnetics Society (ACES) Journal*, vol. 29, no. 10, pp. 793-800, Oct. 2014.

[6] S. C. Basaran, U. Olgun, and K. Sertel, "Multiband monopole antenna with complementary split-ring resonators for WLAN and WiMAX applications," *Electron Lett.*, vol. 49, no. 10, pp. 636-638, May 2013.

[7] N. T. Selvi, P. T. Selvan, S. P. K. Babu, and R. Pandeeswari, "Multiband metamaterial-inspired antenna using split ring resonator," *Computers & Electrical Engineering*, vol. 84, 106613, pp. 1-13, 2020.

[8] A. Sondas, M. H. B. Ucar, and Y. E. Erdemli, "Tunable SRR-based substrate for a microstrip patch antenna," *Turk. J. Elec. & Eng. Comp. Sci.*, vol. 20, no. 1, pp. 159-168, Jan. 2012.

[9] W. Cao, W. Ma, W. Peng, and Z. N. Chen, "Bandwidth-enhanced electrically large microstrip antenna loaded with SRR structures," *IEEE Antennas Wireless Propagat. Lett.*, vol. 18, no. 4, pp. 576-580, Apr. 2019.

[10] A. Sharma, D. Gangwar, K. B. Kumar, and S. Dwari, "RCS reduction and gain enhancement of SRR inspired circularly polarized slot antenna using metasurface," *AEU - International Journal of Electronics and Communications*; vol. 91, pp. 132-142, May 2018.

[11] D. Kaushal and T. Shanmuganantham, "Parametric enhancement of a novel microstrip patch antenna using circular SRR loaded fractal geometry," *Alexandria Engineering Journal*, vol. 57, no. 4, pp. 2551-2557, Dec. 2018.

[12] T. Yue, Z. H. Jiang, A. H. Panaretos, and D. H. Werner, "A compact dual-band antenna enabled by a complementary split-ring resonator-loaded metasurface," *IEEE Trans. Antennas Propagat.*, vol. 65, no. 12, pp. 6878-6888, Dec. 2017.

[13] M. Rezvani and Y. Zehforoosh, "A dual-band multiple-input multiple-output microstrip antenna

with metamaterial structure for LTE and WLAN applications," *AEU - International Journal of Electronics and Communications*, vol. 93, pp. 277-282, Sept. 2018.

[14] B. Urul, "Gain enhancement of microstrip antenna with a novel DNG material," *Micro. Opt. Technol. Lett.*, vol. 62, no. 4, pp. 1824-1829, Jan. 2020.

[15] P. K. Panda and D. Ghosh, "Isolation and gain enhancement of patch antennas using EMNZ superstrate," *AEU - International Journal of Electronics and Communications*, vol. 86, pp. 164-170, Mar. 2018.

[16] J. A. Brown, S. Barth, B. P. Smyth, and A. K. Tyer, "Dual-band microstrip corporate feed network using an embedded metamaterial-based EBG," *IEEE Trans. Antennas Propagat.*, vol. 67, no. 11, pp. 7031-7039, Nov. 2019.

[17] B. A. Mouris, A. Fernandez-Prieto, R. Thobaben, J. Martel, F. Mesa, and O. Quevedo-Teruel, "On the increment of the bandwidth of mushroom-type EBG structures with glide symmetry," *IEEE Trans. Microw. Theory Tech.*, vol. 68, no. 4, pp. 1365-1375, Apr. 2020.

[18] T. K. Das, B. Dwivedy, and S. K. Behera, "Design of a meandered line microstrip antenna with a slotted ground plane for RFID applications," *AEU-International Journal of Electronics and Communications*, vol. 118, 153130, pp. 1-7, May 2020.

[19] N. Pouyanfar, C. Ghobadi, and J. Nourinia, "A compact multi-band MIMO antenna with high isolation for C and X bands using defected ground structure," *Radioengineering*, vol. 27, no. 3, pp. 686-693, Sept. 2018.

[20] J. B. Pendry, A. J. Holden, D. J. Robbins, and W. J. Stewart, "Magnetism from conductors and enhance nonlinear phenomena," *IEEE Trans. Microw. Theory Tech.*, vol. 47, no. 11, pp. 2075-2084, Nov. 1999.

[21] F. Falcone, T. Lopetegi, M. A. G. Laso, J. D. Baena, J. Bonache, M. R. Beruete, F. Martin, and M. Sorolla, "Babinet principle applied to the design of metasurfaces and metamaterials," *Phys. Rev. Lett.*, vol. 93, no. 19, 197401, pp. 1-4, Nov. 2004.

[22] F. Falcone, T. Lopetegi, J. D. Baena, R. Marques, F. Martin, and M. Sorolla, "Effective negative-ε stopband microstrip lines based on complimentary split ring resonators," *IEEE Microwave and Wireless Component Letters*, vol. 14, no. 6, pp. 280-282, June 2004.

[23] CST Microwave Studio, ver. 2008, Computer Simulation Technology, Framingham, MA, 2008.

[24] X. Chen, T. M. Grzegorczyk, B. I. Wu, J. Pacheco Jr, and J. A. Kong, "Robust method to retrieve the constitutive effective parameters of metamaterials," *Phys. Rev.-E*, vol. 70, no. 1, 016608, pp. 1-7, July 2004.

Mustafa Hikmet Bilgehan Ucar was born in Istanbul, Turkey, in 1982. He received his B.S., M.S., and Ph.D. degrees from Kocaeli University, Kocaeli, Turkey, all in Electronics and Computer Education Department in 2004, 2007, and 2013, respectively. He currently serves as an Assistant Professor in the Department of Information Systems Engineering, Kocaeli University, Turkey. His main research interests include numerical analysis and design of reconfigurable antennas/arrays/EM filters and frequency selective surfaces for various communication applications. His research also focuses on embedded systems, user interface design and its usability.